November 1993

JEF/DOC-459

Benchmark Testing of the EJ2-XMAS Library by PASC-4 Code System

(Discussion paper)

Wang Yaoqing †

† Guest from the Institute of Atomic Energy, Chinese Nuclear Data Center, Beijing, P.R.China

Abstract

The JEF2.2 evaluated nuclear data library was issued by the OECD NEA data bank in 1991. At ECN, it has been employed to generate a EJ2-XMAS 172 group neutron library. For the validation of the EJ2-XMAS library, a number of CSEWG (Cross Section Evaluation Working Group) thermal reactor benchmarks, which include ORNL-1 through 4 and 10, TRX-1 through 4 and BAPL-UO_2-1 through 3, have been calculated by PASC-4 code system with EJ2-XMAS library.

This paper presents the results of the benchmark calculations. By comparing the results between EJ2-XMAS and IJ1-XMAS, the differences on ^{16}O cross sections from the evaluated data libraries JEF1.1 and JEF2.2 are discussed.

Results obtained with the EJ2-XMAS show a good agreement with the experimental values and are comparable with those from ENDF/B-V.

1 Introduction

The JEF2.2 evaluated nuclear data library was issued by the OECD NEA data bank in 1991. This library is used to generate a 172 XMAS group structure library in the AMPX master format called EJ2-XMAS. For the validation of the EJ2-XMAS library, a number of CSEWG thermal reactor benchmarks, which include ORNL-1 through 4 and 10, TRX-1 through 4, and BAPL-UO_2-1 through 3, were calculated using the PASC-4 code system. PASC-4 is developed as an intermediate step towards the new code system fully based on SCALE4.

In order to compare the results, the IJ1-XMAS library has also been used to calculate those benchmarks too. This is because the EJ2-XMAS and IJ1-XMAS libraries have the same group structure and are generated by the same NJOY-MILER code system. Their difference is only that the IJ1-XMAS library is based on JEF1.1 and processed by IRI, Delft; while the EJ2-XMAS library is based on JEF2.2 and processed by ECN.

This paper describes the results of the benchmark calculations. On the other hand, through the comparisons of the results between EJ2-XMAS and IJ1-XMAS, the differences on ^{16}O cross sections from the different evaluated data libraries JEF1.1 and JEF2.2 are discussed in this paper too.

On the whole, the EJ2-XMAS results show a good agreement with the experimental values and are comparable with those from ENDF/B-V.

2 EJ2-XMAS Library Generation

The $NJOY_{89.62}$ [1] and MILER-4 [2] codes have been used to generate the EJ2-XMAS library in the 172 XMAS group structure as defined in JEF-DOC-315. The multigroup constant processing code system is shown in Figure 1.

The NJOY modules RECONR, BROADR, THERMR, UNRESR and GROUPR were applied to treat the JEF2.2 evaluated nuclear data for each nuclide to get GENDF output. In this step, the nuclides were processed at several different σ_0 (barn) and temperature (K) values. The weighting spectrum for group averaging is Maxwellian+1/E+Fission with the following parameters :

$E_{therm.max}$=0.025 eV corresponding to a temperature of 293.6 K

$E_{therm.break}$=0.100001 eV

$E_{fiss.break}$=0.820850 MeV

$E_{fiss.max}$=1.4 MeV.

Upper energy limit of the thermal treatment is 3.30 eV.

Legendre order for the anisotropic scattering is P_3.

MILER-4 is an extensively revised version of the original MILER code [3]. It converts the NJOY GENDF format to AMPX master format and passes the resolved resonance parameters from the evaluated nuclear data library (JEF2.2) to the AMPX master library. In this case the Bondarenko factors are set to 1 in the resolved energy range. Thus, the EJ2-XMAS library contains Bondarenko factors in the unresolved resonance region and resonance parameters in the resolved resonance region for nuclides having both resolved and unresolved resonance regions.

The EJ2-XMAS library is suitable for use in the PASC-4 code system, which treats the resonance self-shielding by the Bondarenko method for the unresolved resonance region and by the Nordheim method for the resolved resonance region.

Details about the EJ2-XMAS library generation are given in ref.[4].

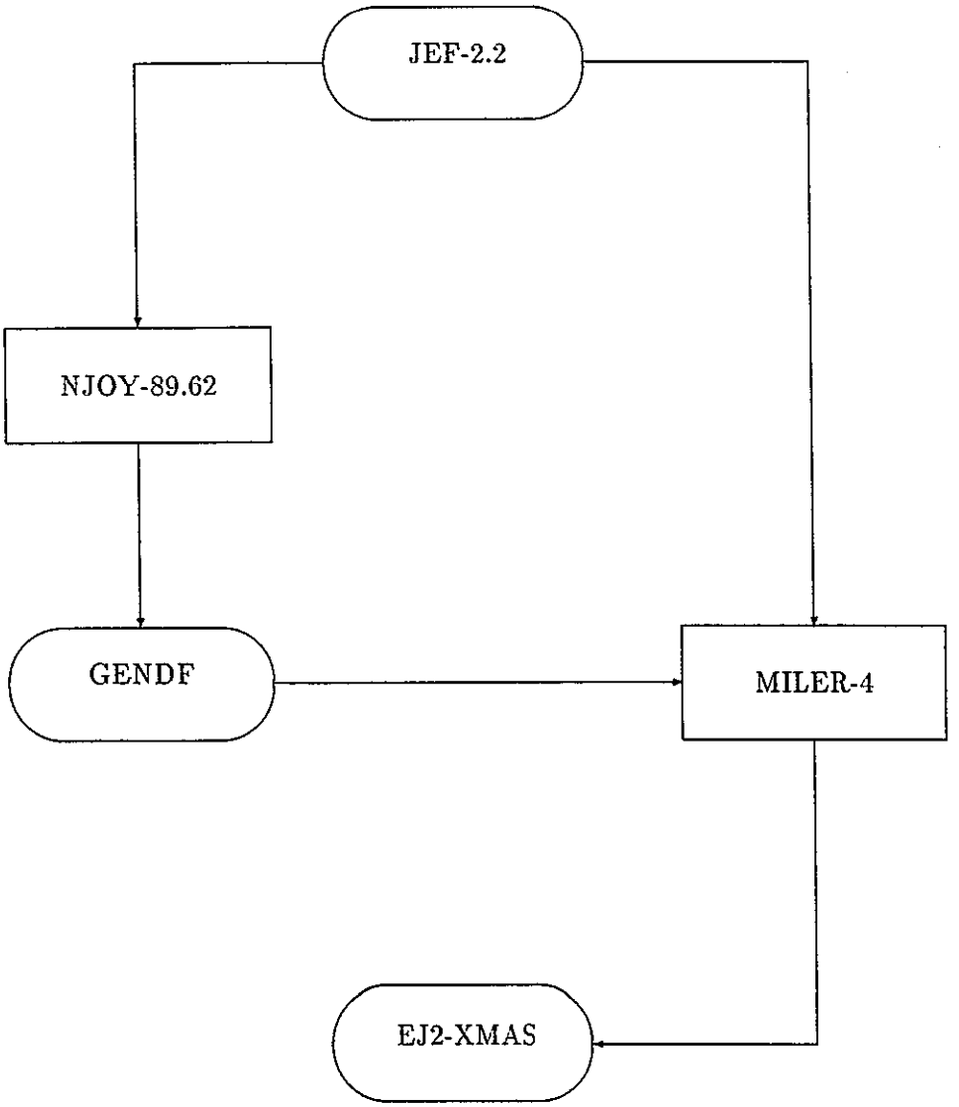

Figure 1 : ECN code system for multigroup cross section generation.

3 The PASC Code System

PASC (Petten-Ampx-SCale) is a reactor physics calculational code system. Most of the modules and codes of PASC originate from the Oak Ridge National Laboratory AMPX [5] and SCALE [6] packages, complemented with a number of additional codes. The first version PASC (PASC-1 [7]) consisted of a part of the AMPX and SCALE modules, CITATION, ANISN and DOT3.5, and operated on a CYBER computer with NOS/BE operating system. The PASC-2 package [8] was the same as the PASC-1 package, but operated with CYBER-NOS/VE system. PASC-3 [9] has been developed into a large system which contains not only most of the functional modules of AMPX and SCALE-3, but also drivers and input-processors such as CSAS1 and SAS2. PASC-3 runs under the UNIX operating system on a network of SUN3 and SUN4 workstations and on a CONVEX-C230 supercomputer. All versions of the PASC system have been contributed to the OECD NEA data bank for distribution.

PASC-4 contains a minimum of changes to the PASC-3 system which were necessary for the use of the new representation of the resonances in the EJ2-XMAS library. Figure 2, 3 and 4 are the flowcharts with the PASC-4 modules used in the benchmark calculations, which run on SUN4 workstations.

The functions of modules shown in Figure 2 to 4 are as follows:

AJAX: selects nuclides from AMPX master binary libraries to generate a small master library containing only that data needed for the problem to be calculated.

BONAMI-4: accesses an AMPX master data set that contains Bondarenko factors and performs the resonance self-shielding calculations based on the Bondarenko method to produce a problem-dependent master library. In the PASC-4 code system it is only used to treat self-shielding for the unresolved resonance region.

NITAWL-4: performs a problem-dependent resonance self-shielding calculations by applying the Nordheim integral treatment for the resolved resonance region and produces an AMPX working library. NITAWL-4 is equal to NITAWL-II of SCALE-4, which is an improved version of the original NITAWL. The main improvement is p-wave level resonance treatment, in addition to only s-wave resonance treatment in the original NITAWL.

XSDRNPM: is a one-dimensional discrete ordinates transport code. It can solve infinite slab, cylindrical and spherical geometry problems. It is also a spectrum-averaging code to collapse fine group cross sections to broad group cross sections by spatial spectrum weighting. The output of broad group cross sections can be in the AMPX weighted, ANISN or CCCC format.

CSAS1 (Criticality Safety Analysis Sequence No.1 of SCALE): is a driver module which allows the user to make a cell calculation in one step and with a simplified input file. In other words, it can produce the input files for the BONAMI, NITAWL and XSDRNPM codes, and call them subsequently for execution. If the CSAS1 driver is not used, input files for these modules should be provided manually in the job card.

JAWS: several AMPX-Working libraries can be combined into one Working library by JAWS.

KENO.5A: is a Monte Carlo code.

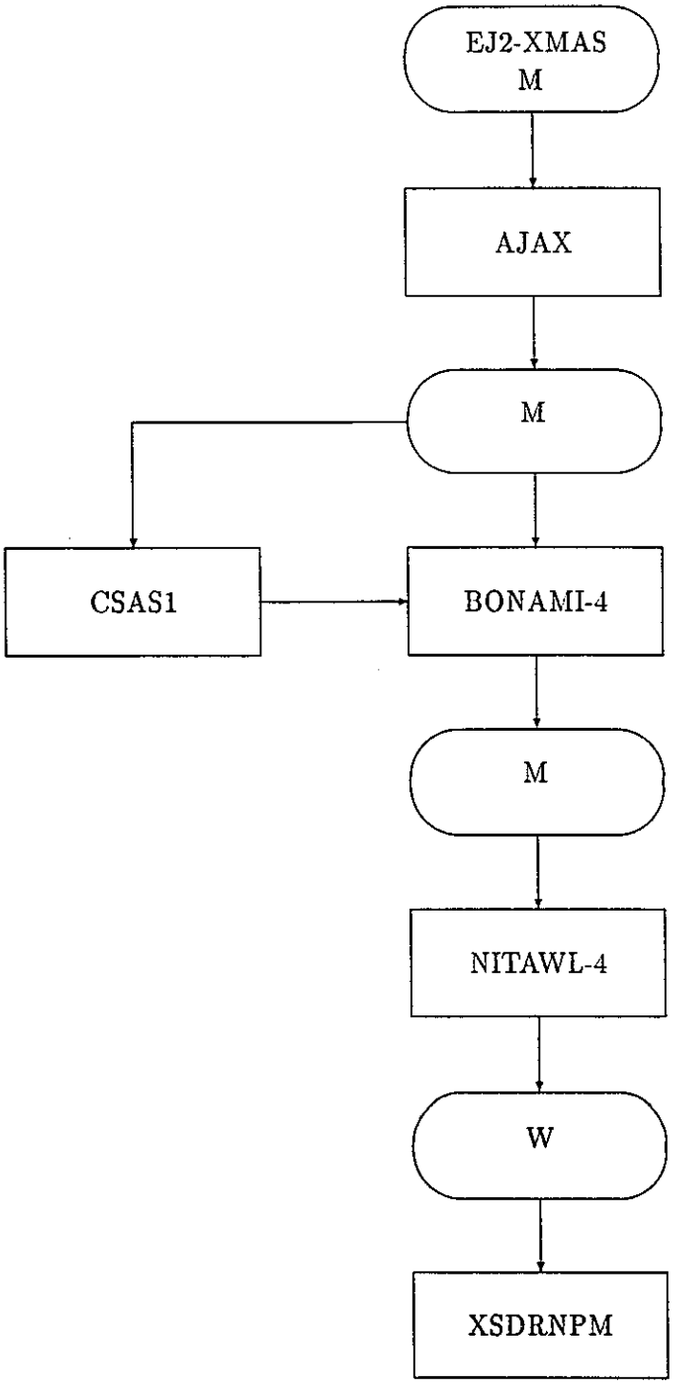

Figure 2: Flowchart 1 of the PASC-4 modules used for ORNL benchmark calculations.

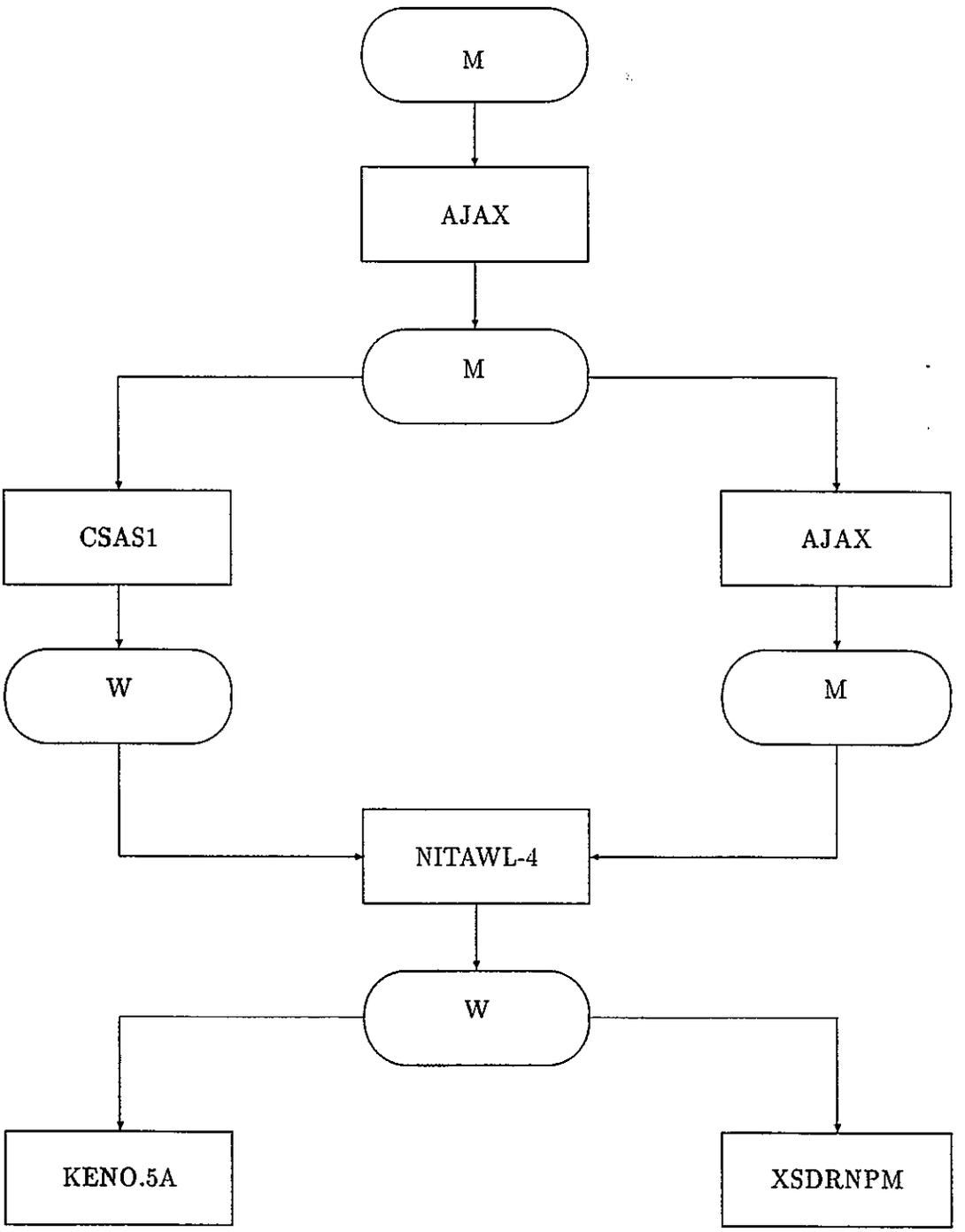

Figure 3 : Flowchart 2 of the PASC-4 modules used for TRX-1, 2 and BAPL benchmark calculations

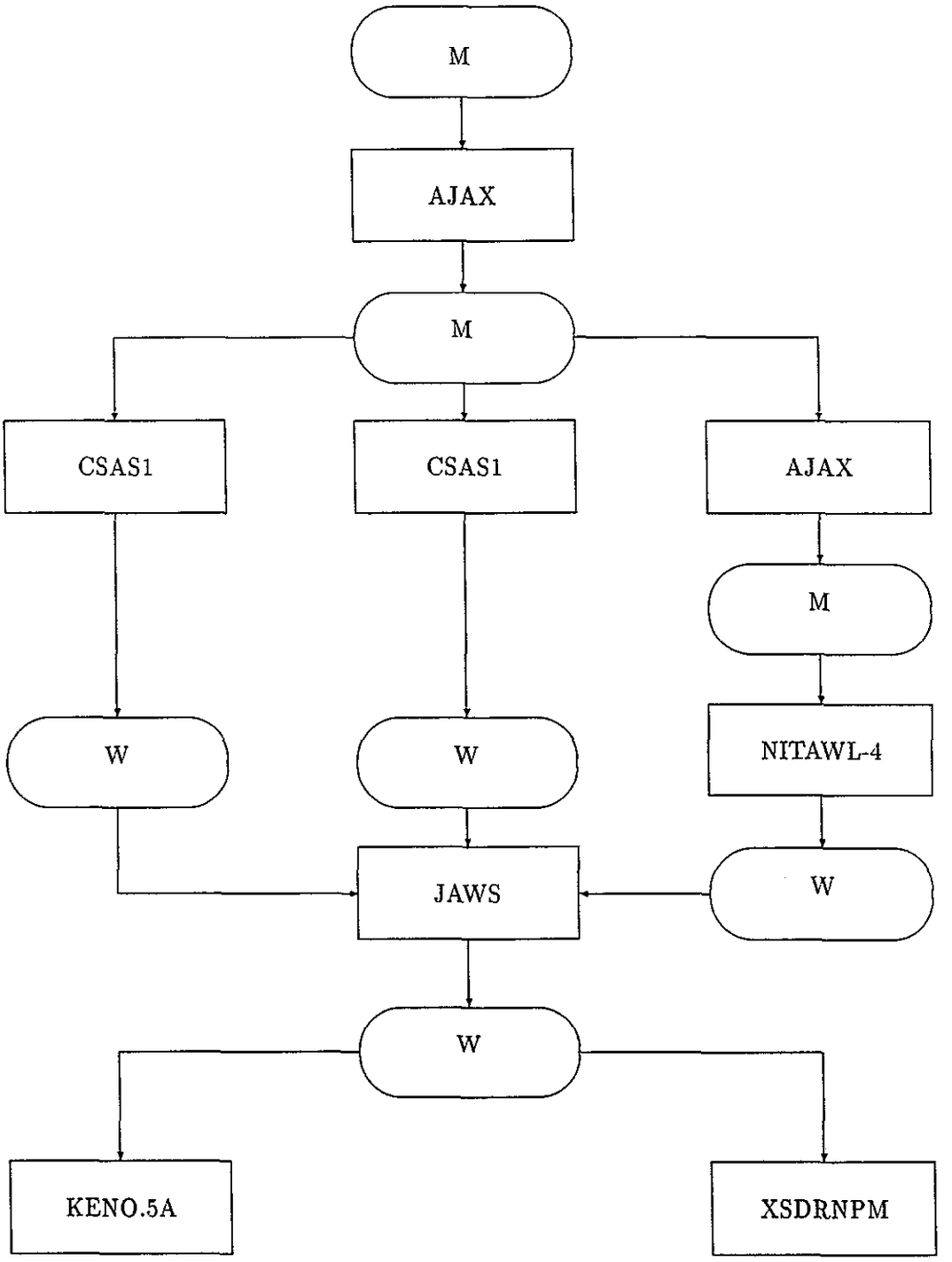

Figure 4 : Flowchart 3 of the PASC-4 modules used for TRX-3 and 4 benchmark calculations

4 Definition of Benchmark Assemblies

(1). ORNL-1, 2, 3, 4 and 10

ORNL-1, 2, 3, 4 and 10 are specified by CSEWG as benchmark assemblies for thermal system with highly enriched uranium. Ref.[11] gives a full description for them. The benchmarks are homogeneous and unreflected spheres of U-235 (as uranyl nitrate) in H_2O, three of them poisoned with boron. Benchmarks ORNL-1 through ORNL-4 are of radius 34.595 cm; ORNL-10 has radius 61.011 cm. The atomic densities of the different isotopes are listed in Table 1.

Table 1: Densities of the different isotopes of the thermal benchmarks ORNL-1, 2, 3. 4 and 10

concentration, 10^{24} atoms/cm^3					
Material	ORNL-1	ORNL-2	ORNL-3	ORNL-4	ORNL-10
^{10}B	0.0	1.0286×10^{-6}	2.0571×10^{-6}	2.5318×10^{-6}	0.0
H	0.066228	0.066148	0.066070	0.066028	0.066394
O	0.033736	0.033800	0.033865	0.033902	0.033592
N	1.869×10^{-4}	2.129×10^{-4}	2.392×10^{-4}	2.548×10^{-4}	1.116×10^{-4}
^{234}U	5.38×10^{-7}	6.31×10^{-7}	7.16×10^{-7}	7.62×10^{-7}	4.09×10^{-7}
^{235}U	4.8066×10^{-5}	5.6206×10^{-5}	6.3944×10^{-5}	6.7959×10^{-5}	3.6185×10^{-5}
^{236}U	1.38×10^{-7}	1.63×10^{-7}	1.84×10^{-7}	1.97×10^{-7}	2.20×10^{-7}
^{238}U	2.807×10^{-6}	3.281×10^{-6}	3.734×10^{-6}	3.967×10^{-6}	1.985×10^{-6}
H/^{235}U	1378	1177	1033	972	1835

(2) TRX-1, 2, 3 and 4

These are H_2O-moderated, fully reflected simple assemblies operated at room temperature. The fuel rods consist of uranium metal (enriched to 1.3 % U-235) cladded in aluminium. They are 48 inches long and 0.387 inch in diameter and arranged in triangular lattices. TRX-1 and TRX-2 are uniform lattices with moderator/fuel volume ratios of 2.35 and 4.02, respectively. TRX-3 and TRX-4 are two-region assemblies in which the test lattice is surrounded by a driver of UO_2 rods. The moderator/fuel volume ratios are 1.00 and 8.11 respectively.
The physical properties of the lattices are given in Tables 2. 3 and 4, in which all data are from ref.[11].
The measured lattice parameters of the critical systems include :

- ρ^{28} : ratio of epithermal-to-thermal ^{238}U capture reaction rates.
- δ^{25} : ratio of epithermal-to-thermal ^{235}U fission reaction rates.
- δ^{28} : ratio of ^{238}U to ^{235}U fission reaction rates.
- C* : ratio of ^{238}U captures to ^{235}U fission reaction rates.

Table 2: Physical Properties of Uranium Metal Lattice

Region	Outer Radius, cm	Isotope	Concentration, 10^{24} Atoms/cm^3
Fuel	0.4915	^{235}U	6.253×10^{-4}
		^{238}U	4.7205×10^{-2}
Void	0.5042		
Clad	0.5753	^{27}Al	6.025×10^{-2}
Moderator	*	^{1}H	6.676×10^{-2}
		^{16}O	3.338×10^{-2}

* Lattice spacings of 1.8060, 2.1740, 1.4412, and 2.8824 cm respectively, for TRX-1 through TRX-4.

Table 3: Propertics of UO_2 Driver Lattice (TRX-3 and TRX-4)

Region	Outer Radius, cm	Isotope	Concentration, 10^{24} Atoms/cm^3
Fuel	0.4864	^{235}U	3.112×10^{-4}
		^{238}U	2.3127×10^{-2}
		^{16}O	4.6946×10^{-2}
Void	0.5042		
Clad	0.5753	^{27}Al	6.025×10^{-2}
Moderator	*	^{1}H	6.676×10^{-2}
		^{16}O	3.338×10^{-2}

*Triangular pitch lattice with spacing of 1.8060 cm

Table 4: Dimensions of Cylinderized TRX Lattices

Composition	Outer Radius (cm)			
	TRX-1	TRX-2	TRX-3	TRX-4
Homogenized test lattice cells	26.2093	27.4419	11.1467	11.8198
Water gap	-	-	12.3268	12.3268
Homogenized driver lattice cells	-	-	37.9406	42.1717
Reflector	-large-			

(3). BAPL-UO_2-1, 2 and 3

These are H_2O-moderated, fully reflected simple assemblies operated at room temperature. The fuel rods are of high-density UO_2 (1.3 % ^{235}U) cladded in aluminium. They are 48 inchs long and 0.383 inch in diameter, arranged in triangular lattices with moderator/fuel volume ratios of 1.43, 1.78 and 2.40 respectively.

The physical properties of lattices are given in Table 5, in which all data are from ref.[11].

Table 5: Physical Properties of The Lattice

Region	Outer Radius, cm	Isotope	Concentration, 10^{24} Atoms/cm^3
Fuel	0.4864	^{235}U	3.112×10^{-4}
		^{238}U	2.3127×10^{-2}
		^{16}O	4.6946×10^{-2}
Void	0.5042		
Clad	0.5753	^{27}Al	6.025×10^{-2}
Moderator	*	^{1}H	6.676×10^{-2}
		^{16}O	3.338×10^{-2}

* Triangular lattices with a pitch of 1.5578, 1.6523 and 1.8057 cm respectively, for BAPL-UO_2-1 through BAPL-UO_2-3.

5 Results

(1) ORNL-1, 2, 3, 4 and 10

The ORNL benchmarks are homogeneous assemblies. They were calculated by PASC-4 modules as shown in Fig. 2. The EJ2-XMAS and IJ1-XMAS libraries were used in the calculations. In order to analyse the difference of results calculated using those two libraries, we took the cross sections of ^{16}O from IJ1-XMAS and the other nuclide cross sections from EJ2-XMAS library (Afterwards, it is called EJ2+O16(IJ1) library) to calculate all benchmarks. This is because differences of ^{16}O cross sections were found from the evaluated data libraries JEF2.2 and JEF1.1, which are shown in Fig. 5 to 10. The calculated K_{eff} results are listed in Table 6. In this Table, the results from other studies are given too.

Table 6: Multiplication Factors for ORNL Benchmark Calculations From ECN and Others

Assembly		ORNL-1 H/U235 1378	ORNL-2 H/U235 1177	ORNL-3 H/U235 1033	ORNL-4 H/U235 972	ORNL-10 H/U235 1835	Average
		K_{eff}	K_{eff}	K_{eff}	K_{eff}	K_{eff}	K_{eff}
expermental values		1.00026	0.99975	0.99994	0.99924	1.00031	0.9999
ECN/PASC-4 (XSDRNPM)	EJ2-XMAS[a]	0.99832	0.99800	0.99496	0.99641	0.99801	0.99714
	EJ2+O16(IJ1)[b]	1.0004	1.0001	0.99705	0.99851	0.99944	0.9991
	IJ1-XMAS[c]	1.00130	1.00091	0.99777	0.99919	1.00023	0.99988
ECN/PASC-3[12]	ECNJEF1[d]	1.00133	1.00105	0.99799	0.99947	0.99920	0.99997
IKE/ANISN[13] MATXS library	JEF-1	1.0013	1.0015	0.9987	0.9997	0.9986	0.99996
	JEF-2	0.9989	0.9981	0.9944	0.9959	0.9981	0.99708
LANL[14] MCNP	ENDF/B-IV	1.0005	1.0006	0.9970	0.9982	0.9964	0.99854
	ENDF/B-V	1.0025	1.0020	0.9972	1.0016	0.9977	1.0002

[a]based on JEF2.2 (EJ2-XMAS library processed by ECN).

[b]cross sections of ^{16}O taken from IJ1-XMAS, the other nuclide cross sections taken from EJ2-XMAS.

[c]based on JEF1.1 (IJ1-XMAS library processed by IRI, Delft).

[d]219 group library based on JEF1.

The K_{eff} values averaged over all ORNL assemblies (ORNL-1 through 4 and 10) for the different library are summarized as follows :

EJ2-XMAS : $<K_{eff}> = 0.99714 \pm 0.00128$

EJ2+O16(IJ1) : $<K_{eff}> = 0.9991 \pm 0.00121$

IJ1-XMAS : $<K_{eff}> = 0.99988 \pm 0.00127$

ECNJEF1 : $<K_{eff}> = 0.99981 \pm 0.00153$

IKE/JEF-1 : $<K_{eff}> = 0.99996 \pm 0.00124$

IKE/JEF-2 : $<K_{eff}> = 0.99708 \pm 0.00167$

ENDF/B-IV : $<K_{eff}> = 0.99854 \pm 0.0017$

ENDF/B-V : $<K_{eff}> = 1.0002 \pm 0.00230$

In order to analyse the difference of the results between EJ2-XMAS and IJ1-XMAS, the reaction rates are calculated for ORNL-1, which are listed in Table 7 and 8.

Table 7: Neutron balance breakdown (ORNL-1 benchmark) under k_∞ calculation

	IJ1-XMAS			EJ2-XMAS			EJ2+O16(IJ1)		
	Absorption	Fission	Neutron Yield	Absorption	Fission	Neutron Yield	Absorption	Fission	Neutron Yield
H	4.017E-1			4.016E-1			4.020E-1		
N14	6.693E-3			6.691E-3			6.698E-3		
O16	3.279E-3			4.256E-3			3.236E-3		
U234	1.245E-3	1.118E-5	2.837E-5	1.244E-3	1.119E-5	2.839E-5	1.246E-3	1.120E-5	2.842E-5
U235	5.863E-1	4.984E-1	1.214520	5.855E-1	4.974E-1	1.212710	5.861E-1	4.980E-1	1.21396
U236	4.865E-5	1.321E-6	3.356E-6	4.859E-5	1.320E-6	3.351E-6	4.865E-5	1.322E-6	3.358E-6
U238	7.032E-4	8.363E-6	2.363E-5	7.011E-4	8.080E-6	2.269E-5	7.021E-4	8.100E-6	2.277E-5
Total	0.999979	0.498391	1.214575	1.000007	0.497451	1.212764	1.000031	0.498021	1.214015

Table 8: Neutron balance breakdown (ORNL-1 benchmark) under K_{eff} calculation

	IJ1-XMAS			EJ2-XMAS			EJ2+O16(IJ1)		
	Absorption	Fission	Neutron Yield	Absorption	Fission	Neutron Yield	Absorption	Fission	Neutron Yield
H	3.311E-1			3.305E-1			3.312E-1		
N14	5.534E-4			5.524E-3			5.536E-3		
O16	2.875E-3			3.732E-3			2.835E-3		
U234	1.036E-3	9.734E-6	2.476E-5	1.037E-3	9.746E-6	2.477E-5	1.036E-3	9.757E-6	2.481E-5
U235	4.835E-1	4.109E-1	1.00125	4.821E-1	4.095E-1	0.998270	4.831E-1	4.103E-1	1.00036
U236	4.154E-5	1.165E-6	2.962E-6	4.143E-5	1.164E-6	2.958E-6	4.153E-5	1.166E-6	2.964E-6
U238	6.032E-4	7.506E-6	2.118E-5	6.006E-4	7.261E-6	2.036E-5	6.020E-4	7.273E-6	2.041E-5
Total	0.819709	0.410918	1.001299	0.823535	0.409518	0.998318	0.824351	0.4103182	1.000408

From Table 7 and 8, it can be seen that due to the difference of ^{16}O cross sections between EJ2-XMAS and IJ1-XMAS. the difference of neutron yield rates between them is about 0.2 % for ORNL-1.
As shown in Figures 5 to 10, except the difference of ^{16}O between JEF2.2 and JEF1.1, the scattering cross sections (σ_e and σ_{in}) between them are also differences. which cause the change of the energy spectra and result in the changes of all reaction rates.

(2) TRX-1, 2, 3 and 4

The TRX-Benchmarks are very sensitive to the treatment of the resonances. The modules of PASC-4 used for TRX-1 and 2 are shown in Fig. 3, in which AJAX is used for selecting nuclides from the library. The cell calculations are executed by CSAS1. As mentioned in Section 2 of this paper, the CSAS1 job includes the unresolved resonance treatment by BONAMI-4, the resolved resonance treatment by NITAWL-4, and one-dimensional S_n calculations by XSDRNPM with S_8P_3 (the K_{eff} difference between S_8P_3 and $S_{16}P3$ is less than 0.01 %). The Dancoff factor calculations have also been considered in CSAS1 automaticaly [10]. After running CSAS1, the cell-averaged cross sections can be obtained for the consequently core calculations. The cell reaction rates are evaluated too. For the reflector material (H_2O), no special treatment is needed; so their nuclide cross sections are selected with a second AJAX run and pass to the final criticality calculation. The working library generated by CSAS1 for fuel are combined with the master library for reflector by NITAWL-4.

In the last step XSDRNPM performs a criticality calculation for the whole reactor system with a one-dimensional cylindrical model; the axial leakage is taken into account by the axial buckling correction, using the measured axial buckling (5.26 m^{-2}).

TRX-3 and TRX-4 are two-zone cores, which are central zone uranium metal lattices surrounded by a uranium oxide driver zone. In that case, the CSAS1 is respectively executed for a uranium metal and a uranium oxide driver lattices calculations. The modules of PASC-4 used for TRX-3 and 4 are shown in Fig. 4, in which the second AJAX run is to select the nuclide cross sections contained in reflector material (H_2O) and the NITAWL-4 here is only is used for translating Master format library into Working library. Then three working libraries are combined by the JAWS. The other steps are the same as mentioned above.

The calculated results are listed in Tables 9, 10, 11 and 12. Those obtained by other studies are also listed in those Tables.

As shown in Fig. 3 and 4, the full core calculations for TRX assemblies were also performed by Monte Carlo code KENO.5A. But those were carried out only by means of EJ2-XMAS library, not by other libraries, because Monte Carl calculations take a long computer time. The K_{eff} values from KENO.5A calculations are listed in Table 16, which are compared with the results calculated by XSDRNPM and will be mentioned in detail late.

Table 9: Integral Parameters for TRX-1

Parameter		k_{eff}	ρ^{28}	δ^{25}	δ^{28}	C*
Experiment		1.000	1.320±0.021	0.0987±0.001	0.0946±0.0041	0.797±0.008
ECN/PASC-4 (XSDRNPM)	EJ2-XMAS	0.9974	1.3260	0.0962	0.092	0.7937
	EJ2+O16(IJ1)	0.9988	1.3254	0.0962	0.092	0.7936
	IJ1-XMAS	1.0001	1.3381	0.0966	0.0941	0.7938
ECN/PASC-3[15]	ECNJEF1.1[a]	0.9968	1.3266	0.0950	0.0962	0.7913
IKE[16]	JEF-1	0.9960	1.3569	0.0992	0.1001	0.7984
ENDF-311[14]	ENDF/B-IV	0.9876	1.3820	0.0994	0.0955	0.8060
ENDF-311	ENDF/B-V	0.9961	1.3590	0.1003	0.0983	0.7980

[a]ECNJEF1.1 is a 219 group library based on JEF1.1

The K_{eff} values averaged over TRX-1 through TRX-4 from the calculations based on different library are summarized as follows :

EJ2-XMAS : $<K_{eff}> = 0.9963 \pm 0.0029$
EJ2+O16(IJ1) : $<K_{eff}> = 0.9978 \pm 0.0030$
IJ1-XMAS : $<K_{eff}> = 0.9991 \pm 0.0029$
ECNJEF1.1 : $<K_{eff}> = 0.9945 \pm 0.0023$
IKE/JEF-1 : $<K_{eff}> = 0.9981 \pm 0.0021$
ENDF/B-IV : $<K_{eff}> = 0.9914 \pm 0.0029$
ENDF/B-V : $<K_{eff}> = 0.9973 \pm 0.0016$ (averaged only over TRX-1 and -2)

(3) BAPL-UO_2-1, 2 and 3

As the same step as TRX-1 and 2 calculations, the modules of PASC-4 shown in Fig. 3 are also used for BAPL-UO_2-1, 2 and 3 benchmark calculations. The results are given in Table 13, 14 and 15. The results from other studies are given too in those Tables.

Table 13: Integral Parameters for BAPL-UO_2-1

Parameter		k_{eff}	ρ^{28}	δ^{25}	δ^{28}	C*
Experiment		1.000±0.00065	1.39±0.01	0.084±0.002	0.078±0.004	-
ECN/PASC-4 (XSDRNPM)	EJ2-XMAS	1.0024	1.4011	0.0818	0.0727	0.8126
	EJ2+O16(IJ1)	1.0043	1.4010	0.0818	0.0727	0.8125
	IJ1-XMAS	1.0054	1.4143	0.0824	0.0749	0.8125
IKE	JEF-1	1.0001	1.4196	0.0841	0.0775	0.8130
ENDF-311	ENDF/B-IV	0.9914	1.447	0.0841	0.0738	0.822
ENDF-311	ENDF/B-V	1.003	1.414	0.084	0.0782	0.810

Table 14: Integral Parameters for BAPL-UO_2-2

Parameter		k_{eff}	ρ^{28}	δ^{25}	δ^{28}	C*
Experiment		1.000±0.00062	1.12±0.01	0.068±0.001	0.070±0.004	-
ECN/PASC-4 (XSDRNPM)	EJ2-XMAS	0.9998	1.1635	0.0667	0.0626	0.7400
	EJ2+O16(IJ1)	1.002	1.1632	0.0667	0.0626	0.7399
	IJ1-XMAS	1.003	1.1745	0.0671	0.0644	0.7394
IKE	JEF-1	0.9999	1.1771	0.0685	0.0668	0.7393
ENDF-311	ENDF/B-IV	0.9932	1.1950	0.0683	0.0633	0.745
ENDF-311	ENDF/B-V	1.0033	1.173	0.0680	0.0653	0.738

In order to analyse the difference of the results calculated with different libraries, the TRX-1 cell and full core spectras are shown in Figure 11 and 12, from which it can be seen that the differences of the spectras between EJ2-XMAS and IJ1-XMAS results are larger in high energy range. Because the differences of $\sigma_{n,\alpha}$, σ_e and σ_{in} between JEF2.2 and JEF1.1 are larger in high energy range, as shown in Figure 8 to 10. The different spectras will cause the different reaction rates and differet K_{eff} values.

Table 10: Integral Parameters for TRX-2

Parameter		k_{eff}	ρ^{28}	δ^{25}	δ^{28}	C*
Experiment		1.000	0.837±0.016	0.0614±0.0008	0.0693±0.0035	0.647±0.006
ECN/PASC-4 (XSDRNPM)	EJ2-XMAS	0.9921	0.8309	0.0592	0.0660	0.6417
	EJ2+O16(IJ1)	0.9933	0.8309	0.0592	0.0660	0.6417
	IJ1-XMAS	0.9948	0.8386	0.0594	0.0678	0.6408
ECN/PASC-3	ECNJEF1.1	0.9923	0.833	0.0588	0.0688	0.6396
IKE	JEF-1	0.9973	0.8374	0.0608	0.0714	0.6393
ENDF-311	ENDF/B-IV	0.9935	0.863	0.0609	0.0676	0.6470
ENDF-311	ENDF/B-V	0.9984	0.846	0.0614	0.0699	0.6420

Table 11: Integral Parameters for TRX-3

Parameter		k_{eff}	ρ^{28}	δ^{25}	δ^{28}	C*
Experiment		1.000	3.03±0.05	0.231±0.003	0.167±0.008	1.255±0.011
ECN/PASC-4 (XSDRNPM)	EJ2-XMAS	0.99998	3.0515	0.2340	0.1673	1.2547
	EJ2+O16(IJ1)	1.0017	3.0510	0.2341	0.1671	1.2545
	IJ1-XMAS	1.0028	3.0839	0.2355	0.1721	1.2596
ECN/PASC-3	ECNJEF1.1	0.9967	3.0486	0.2272	0.1783	1.2546
IKE	JEF-1	1.001	3.013	0.236	0.1725	1.2402
EPRI[17]/WAPD[18]	ENDF/B-IV	0.9908	3.07	0.235	0.174	1.252

Table 12: Integral Parameters for TRX-4

Parameter		k_{eff}	ρ^{28}	δ^{25}	δ^{28}	C*
Experiment		1.000	0.481±0.011	0.0358±0.005	0.0482±0.002	0.531±0.004
ECN/PASC-4 (XSDRNPM)	EJ2-XMAS	0.9957	0.4942	0.0350	0.0492	0.5330
	EJ2+O16(IJ1)	0.9974	0.4942	0.0350	0.0492	0.5330
	IJ1-XMAS	0.9987	0.4986	0.0351	0.0505	0.5314
ECN/PASC-3	ECNJEF1.1	0.9921	0.4891	0.0345	0.0491	0.5288
IKE	JEF-1	0.9979	0.4760	0.0344	0.0473	0.5244
EPRI/WAPD	ENDF/B-IV	0.9937	0.491	0.0345	0.0467	0.5270

Table 15: Integral Parameters for BAPL-UO_2-3

Parameter		k_{eff}	ρ^{28}	δ^{25}	δ^{28}	C*
Experiment		1.000±0.0005	0.906±0.01	0.052±0.001	0.057±0.003	-
ECN/PASC-4 (XSDRNPM)	EJ2-XMAS	0.9953	0.9147	0.0513	0.0517	0.6620
	EJ2+O16(IJ1)	0.9971	0.9145	0.0513	0.0517	0.6619
	IJ1-XMAS	0.9985	0.9233	0.0516	0.0532	0.6609
IKE	JEF-1	0.9988	0.9201	0.0526	0.0549	0.6591
ENDF-311	ENDF/B-IV	0.9940	0.944	0.0523	0.0518	0.667
ENDF-311	ENDF/B-V	1.0045	0.914	0.0525	0.0533	0.656

The K_{eff} values averaged over BAPL-UO_2-1 through 3 from the calculations based on different libraries are summarized as follows :

EJ2-XMAS : $<K_{eff}> = 0.9992 \pm 0.0029$
EJ2+O16(IJ1) : $<K_{eff}> = 1.001 \pm 0.0030$
IJ1-XMAS : $<K_{eff}> = 1.0023 \pm 0.0029$
IKE/JEF-1 : $<K_{eff}> = 0.9996 \pm 0.0007$
ENDF/B-IV : $<K_{eff}> = 0.9929 \pm 0.0013$
ENDF/B-V : $<K_{eff}> = 1.0036 \pm 0.0008$

(4) Comparison of the Results Between KENO.5A and XSDRNPM

In order to compare the results between Monte Carlo and S_n codes, the K_{eff} calculatios for the full cores of the TRX-1 through 4 and BAPL-UO_2-1 through 3 were also performed by KENO.5A. But Monte Carlo calculations take a long computer time, those calculations were carried out only by means of EJ2-XMAS library, without using other libraries.

As shown in Fig. 3 and 4, the working libraries used in XSDRNPM calculation were used in KENO.5A calculatios. The homogeneous cylindrical geometry models were also adopted in KENO.5A calculations, without moking-up the complex real geometry for the full core calculations.

The K_{eff} values from KENO.5A calculations for the TRX-1 through 4 and BAPL-1 through 3 are listed in Tables 16 and 17 respectively. For the comparison, those from XSDRNPM calculations are listed in those Tables too.

Table 16: Comparison of the K_{eff} values calculared by KENO.5A and XSDRNPM with EJ2-XMAS library for TRX assemblies

Code	K_{eff}			
	TRX-1	TRX-2	TRX-3	TRX-4
XSDRNPM	0.9974	0.9921	0.99998	0.9957
KENO.5A	0.9936 ± 0.0037	0.9905 ± 0.0037	0.9968 ± 0.0048	0.9929 ± 0.0048

Table 17: Comparison of the K_{eff} values calculared by KENO.5A and XSDRNPM with EJ2-XMAS library for BAPL-UO_2-1 through 3

Code	K_{eff}		
	BAPL-UO_2-1	BAPL-UO_2-2	BAPL-UO_2-3
XSDRNPM	1.0024	0.9998	0.9953
KENO.5A	1.001 ± 0.0039	0.9974 ± 0.0037	0.9916 ± 0.0038

From Tables 16 and 17, it can be seen that the KENO.5A results agree well with the deterministic XSDRNPM values within the statistical error. The simular difference of the results between Monte Carlo code and other codes (such as S_n) can be found in ref.[13] and [19].

6 Summary and Conclusion

1. A series of CSEWG benchmarks have been tested for the EJ2-XMAS library. The detail results and those from other studies are given in Table 6 to 17. The $<K_{eff}>$ values calculated only by means of EJ2-XMAS library are summarized as follows:

- The $<K_{eff}>$ averaged over ORNL-1 through 4 and 10 is 0.9971 ± 0.0013
- The $<K_{eff}>$ value averaged over TRX-1 through 4 is 0.9963 ± 0.0029
- The $<K_{eff}>$ value averaged over BAPL-UO_2-1 through 3 is 0.9992 ± 0.0029

Those EJ2-XMAS results show a good agreement with the experimental values. The K_{eff} deviations between EJ2-XMAS results and experimental values are less than 0.5 %. In most cases, the EJ2-XMAS results are better than ENDF/B-IV (deviation < 1.0 %) and are comparable with those from ENDF/B-V (deviation < 0.5 %).
The lattice parameters ρ^{28}, δ^{25}, δ^{28} and C* are also in agreement with experimental values and their deviations are comparable with those from other studies.

2. From the comparisons of the results between EJ2-XMAS and IJ1-XMAS, it can be seen that the EJ2-XMAS always gives lower 0.2-0.3 % values for the multiplication factors than IJ1-XMAS. But EJ2+O16(IJ1) always gives the K_{eff} values in those between EJ2-XMAS and IJ1-XMAS. Those are summarized in Table 18 :

Table 18: Comparison of the $<K_{eff}>$ values calculared using different libraries

	$<K_{eff}>$		
averaged over	ORNL-1 through 4 and 10	TRX-1 through 4	BAPL-UO_2-1 through 3
EJ2-XMAS	0.9971	0.9963	0.9992
EJ2+O16(IJ1)	0.9991	0.9978	1.001
IJ1-XMAS	0.99988	0.9991	1.0023

From Table 18, it can be seen that the $<K_{eff}>$ difference between EJ2-XMAS and IJ1-XMAS is about 0.2-0.3 %. Due to the difference of ^{16}O cross sections from both libraries, to cause the difference of $<K_{eff}>$ between them is about 0.15 - 0.2 %.
Through analysing, the differences of ^{16}O cross sections come from the evaluated data libraries JEF1.1 and JEF2.2, which are shown in Figures 5 to 10. Among them, the main difference comes from the different scattering cross sections, the other comes from the different $\sigma_{n,\alpha}$. Because according to alternative calculations, i.e. using $\sigma_{n,\alpha}$ cross sections of JEF1.1 instead of it of JEF2.2 to produce new ^{16}O cross sections of EJ2-XMAS, and then calculating ORNL-4 again, the K_{eff} difference between both EJ2-XMAS libraries is only 0.06 %. So the other 0.1 - 0.15 % K_{eff} difference could come from the different scattering cross sections of ^{16}O in JEF1.1 and JEF2.2. The other differences in the cross sections between both libraries are small.
This is not a serious problem for the EJ2-XMAS or IJ1-XMAS applications. But it is significant for the further evaluation of ^{16}O in future.

References

[1] R.E. MacFarlane, The proceedings of the seminar on NJOY and THEMIS, SACLAY,20-21 June 1989.

[2] P.F.A. de Leege, NSLINK: NJOY-SCALE-LINK, IRI-131-091-003(April 1991).

[3] G.C. Panini, MILER–Master Interface Library makER, Abstract NEA 1198(July 1988).

[4] R.C.L. Van der Stad, Cai Chonghai, H. Gruppelaar and V.L. Lalov Lalov, EJ2-XMAS, A JEF2.2 Based Neutron Cross Section Library in the XMAS Group Structure : User's Manual, ECN report to be published in June, 1993.

[5] N.M. Greene et al., AMPX-2: A Modular Code System for Generating Coupled Neutron-Gamma-Ray Cross-Section Libraries from Data in ENDF Format, ORNL report PSR-63(1984).

[6] SCALE-3.1 A Modular Code System for Performing Standardized Computer Analyses for Licening Evaluation, CCC-466, ORNL(1986).

[7] Wang Yaoqing, J. Oppe, J.B.M. de Haas, H. Gruppelaar, J. Slobben, The Petten AMPX/SCALE Code System PASC-1 for Reactor Neutronics Calculations, ECN-89-005, 1989.

[8] J. Oppe, Changes in Using the PASC-2 on NOS/VE, NFA-LWR-90-08, 1990.

[9] B.J. Pijlgroms, J. Oppe, H. Oudshoorn, The PASC-3 Code System and UNIPASC Environment, ECN-RX-91-078(1991).

[10] SCALE-4: A Modular Code System for Performing Standardized Computer Analyses for Licensing Evaluation, CCC-545, ORNL(1990).

[11] ENDF-202, Cross Section Evaluation Working Group, Benchmark Specification, BNL 19302, New York (Nov. 1974).

[12] J. Oppe, ORNL Benchmarks for 219 Group Library, NFA-LWR-90-14.

[13] W. Bernnat et al., Analysis of Thermal Benchmarks Based on the Evaluated Nuclear Data Files JEF-2 and ENDF/B-VI, Nuclear Data for Science and Technology (1992).

[14] ENDF-311, Benchmark Data Testing of ENDF/B-V, BNL-NCS-31531 (1982).

[15] J. Li. J. Slobben, H. Gruppelaar, TRX Benchmark Test of the PASC-3 Code System and JEF-1 Data Library, NFA-LWR-92-01.

[16] W. Bernnat et al., Analysis of Selected Thermal Reactor Benchmark Experiments Based on the JEF-1 Evaluated Nuclear Data File, IKE 6-157 (1986).

[17] R. Sher et al., Studies of Thermal Reactor Benchmark Data Intepretation : Expermental Correction, EPRI NP-209 (1976)

[18] J. Hardy et al., Monte Carlo Analyses of TRX Slightly Enriched Uranium-H_2O Critical Experiments with ENDF/B-IV and Related Data Sets, WAPD-TM-1307 (1977).

[19] Guidebook for the Conversion from HEU to LEU, IAEA-TECDOC-233 (1980).

Figure 5: Comparison of $\sigma_{n\gamma}$ for ^{16}O between jef1.1 and jef2.2

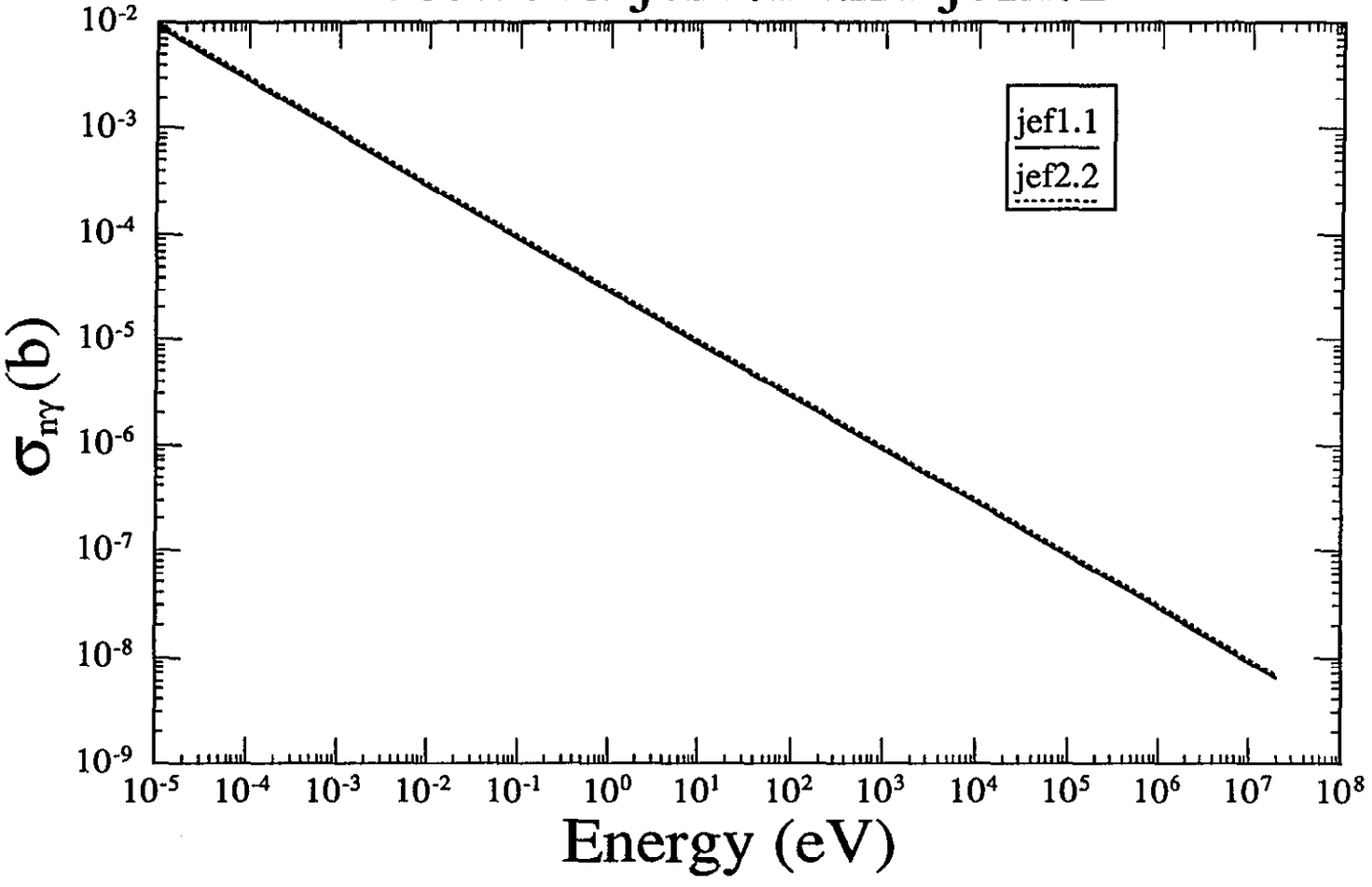

TempleGraph 2.3, Origin: /home/zahir/ywang@crypton - Mon Apr 26 15:08:43 1993 (data file was j2gam)

Figure 6: Comparison of σ_{np} for ^{16}O between jef1.1 and jef2.2

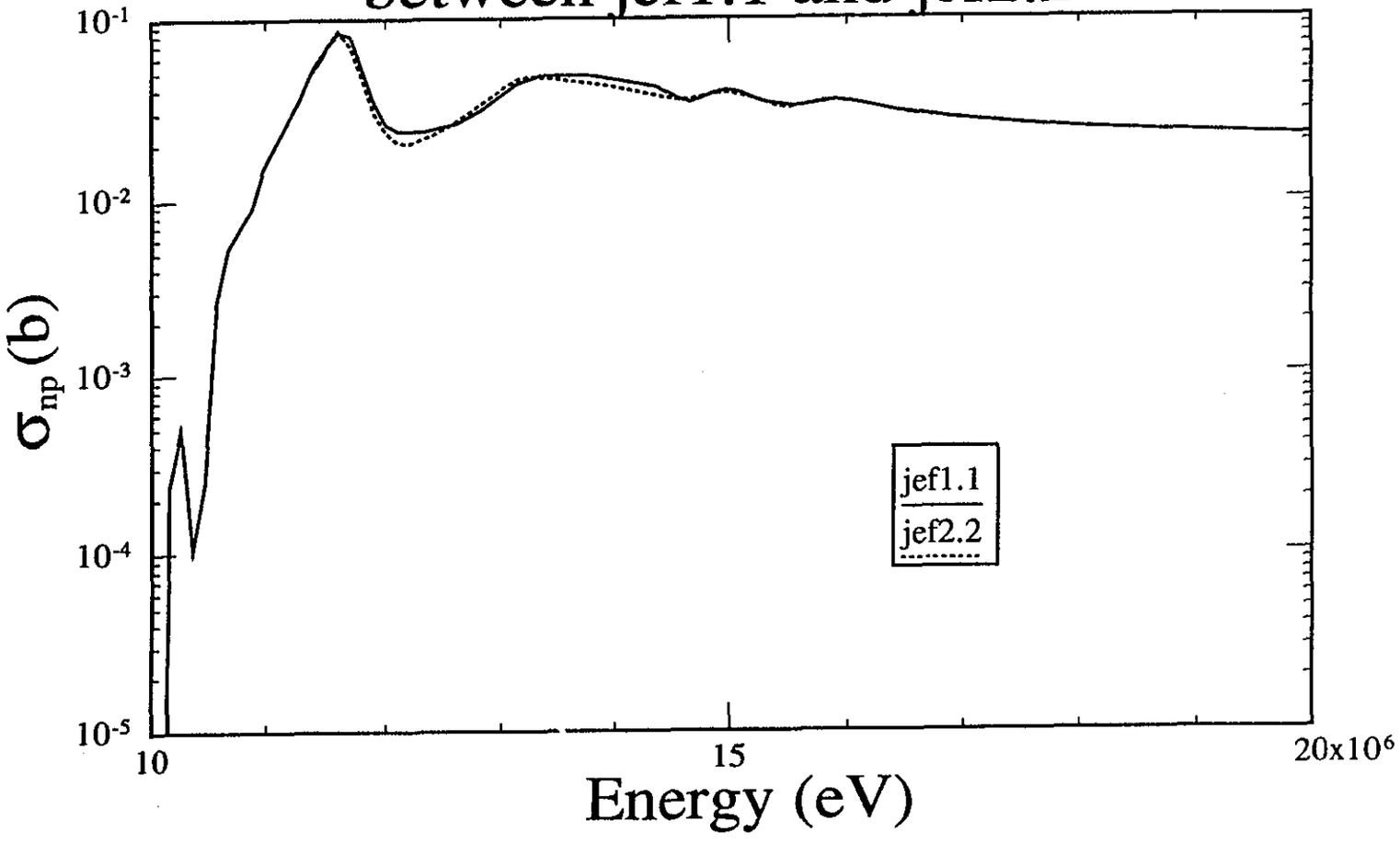

TempleGraph 2.3, Origin: /home/zahir/ywang@crypton - Fri[illegible]r 23 16:53:19 1993 (data file was f2)

Figure 7 : Comparison of σ_{nd} for ^{16}O between jef1.1 and jef2.2

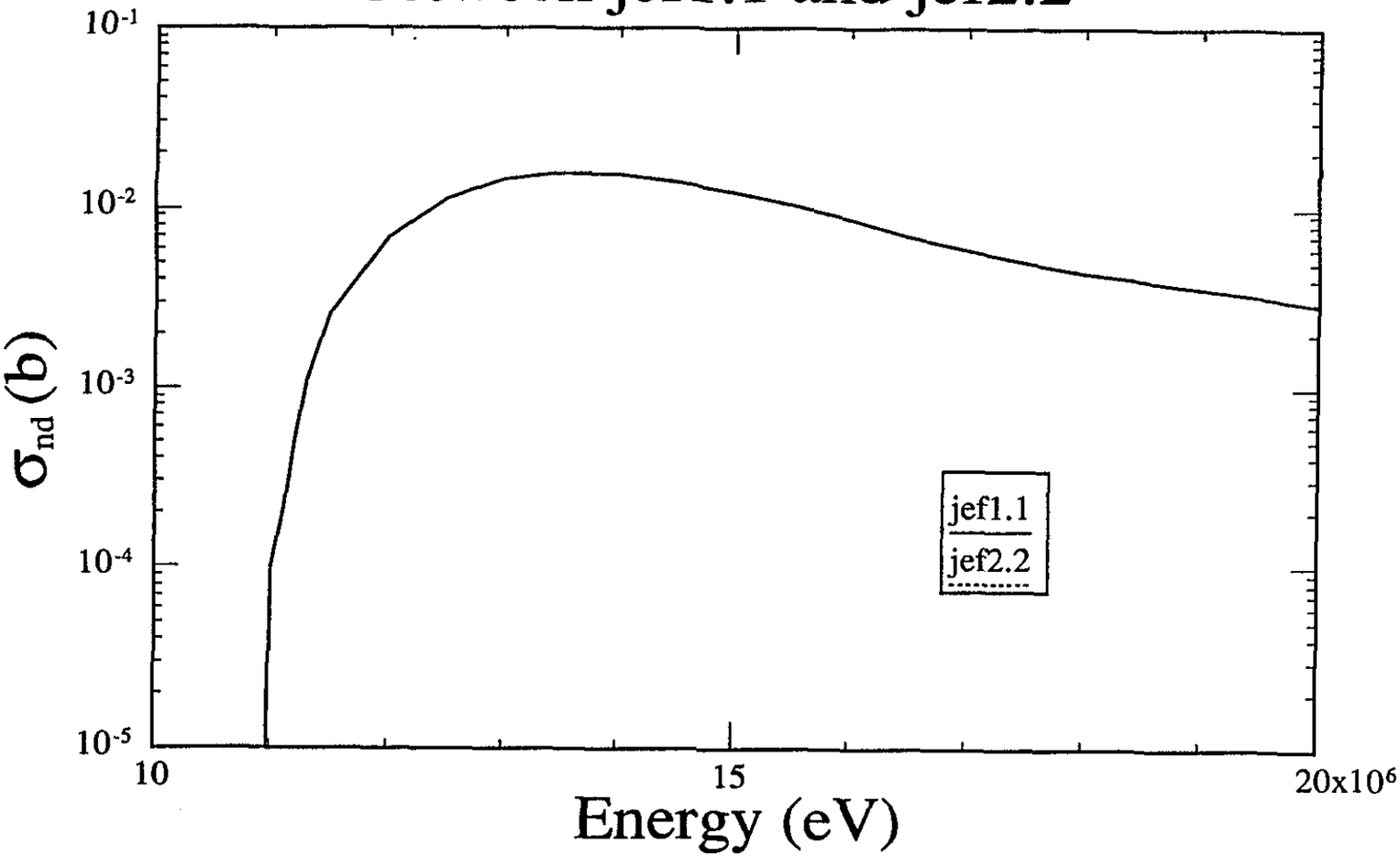

TempleGraph 2.3, Origin: /home/zahir/ywang@crypton - Mon Apr 26 16:42:05 1993 (data file was j2nd)

Figure 8 : Comparison of $\sigma_{n\alpha}$ for ^{16}O between jef1.1 and jef2.2

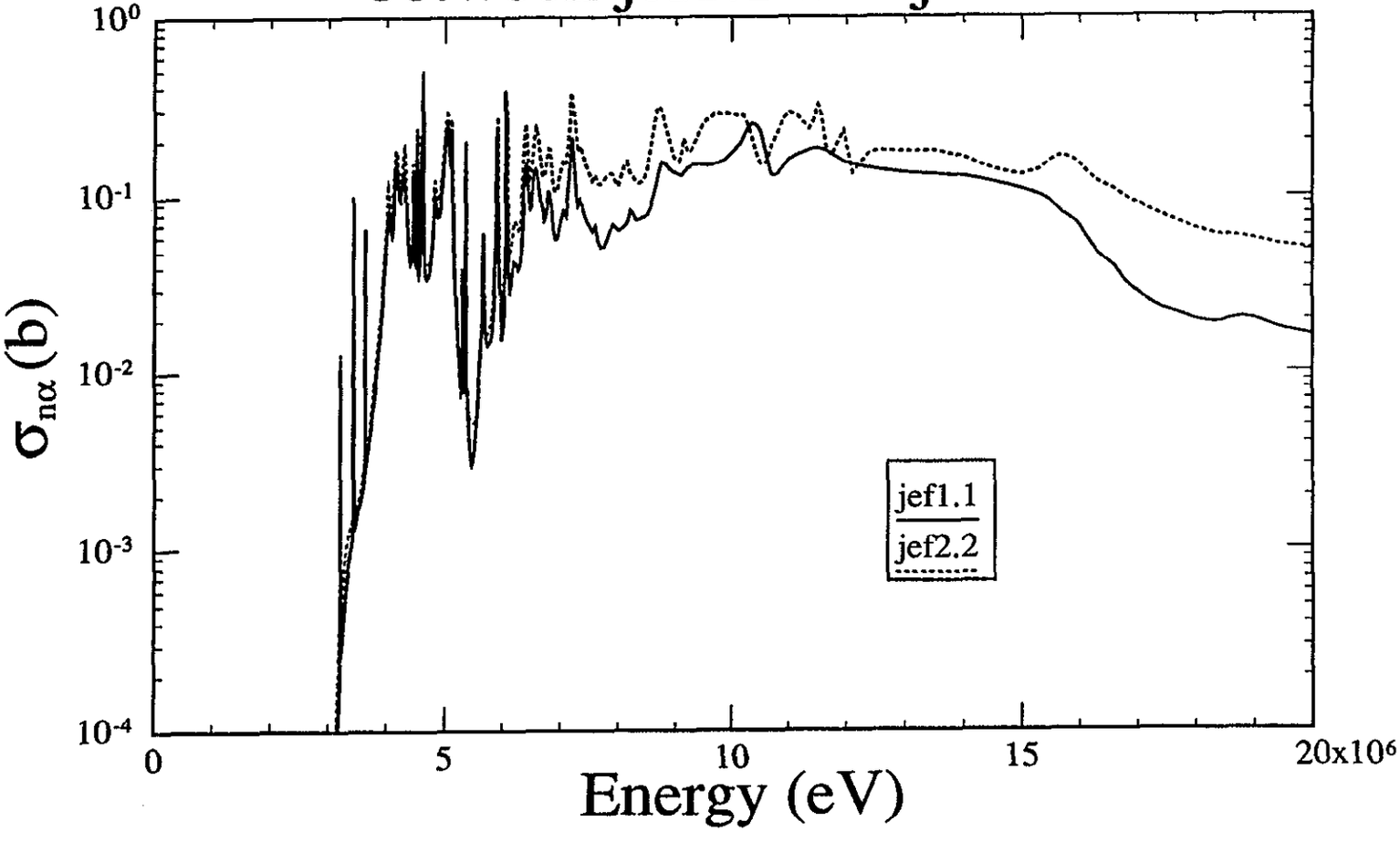

TempleGraph 2.3, Origin: /home/zahir/ywang@crypton - [redacted] Apr 27 16:05:29 1993 (data file was j2pha)

Figure 9 : Comparison of σ_{in} for ^{16}O between jef1.1 and jef2.2

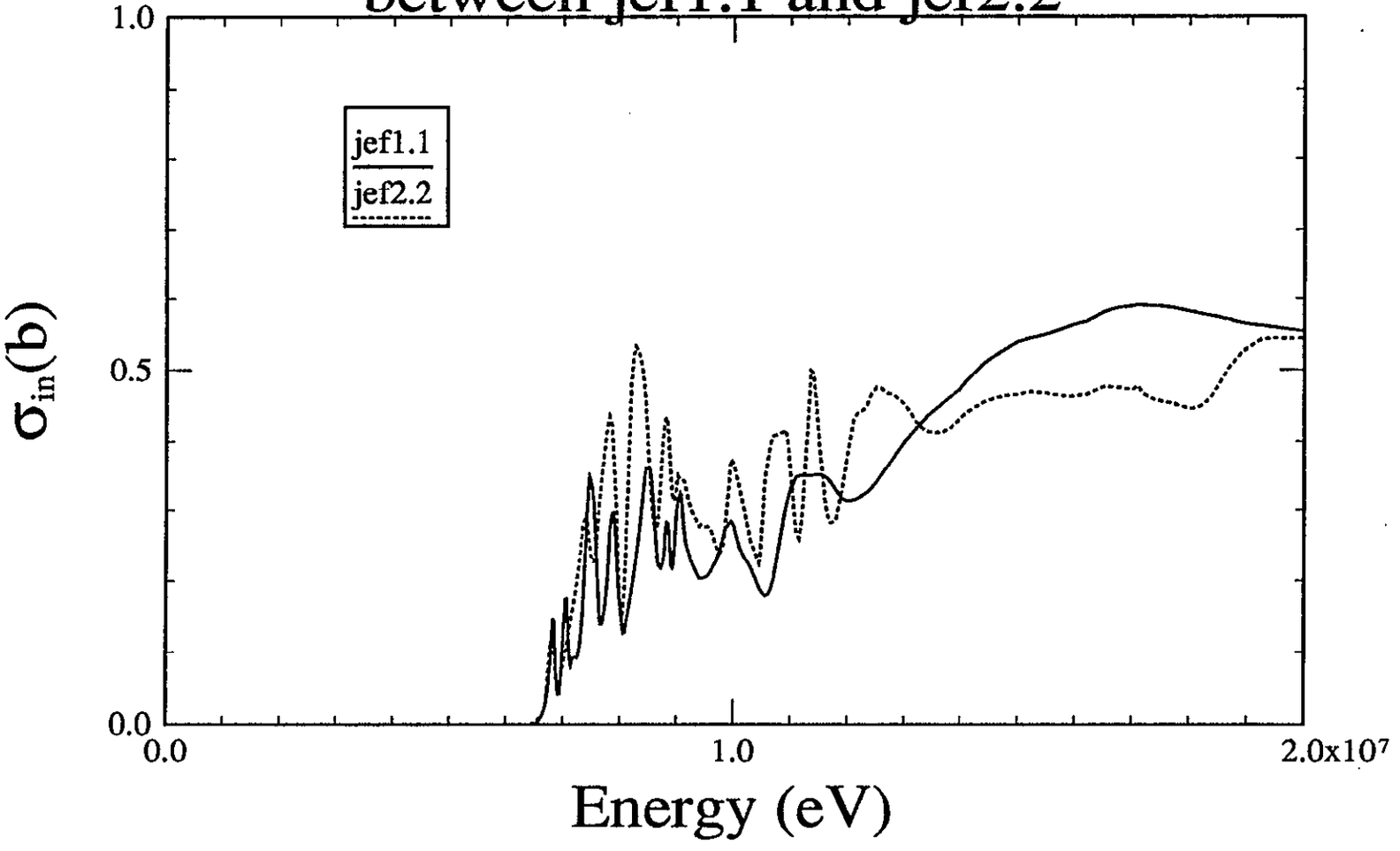

TempleGraph 2.3, Origin: /home/zahir/ywang@zahir - Fri Jul 30 12:18:49 1993 (data file was o16ins)

Figure 10 : Comparison of σ_e for ^{16}O between jef1.1 and jef2.2

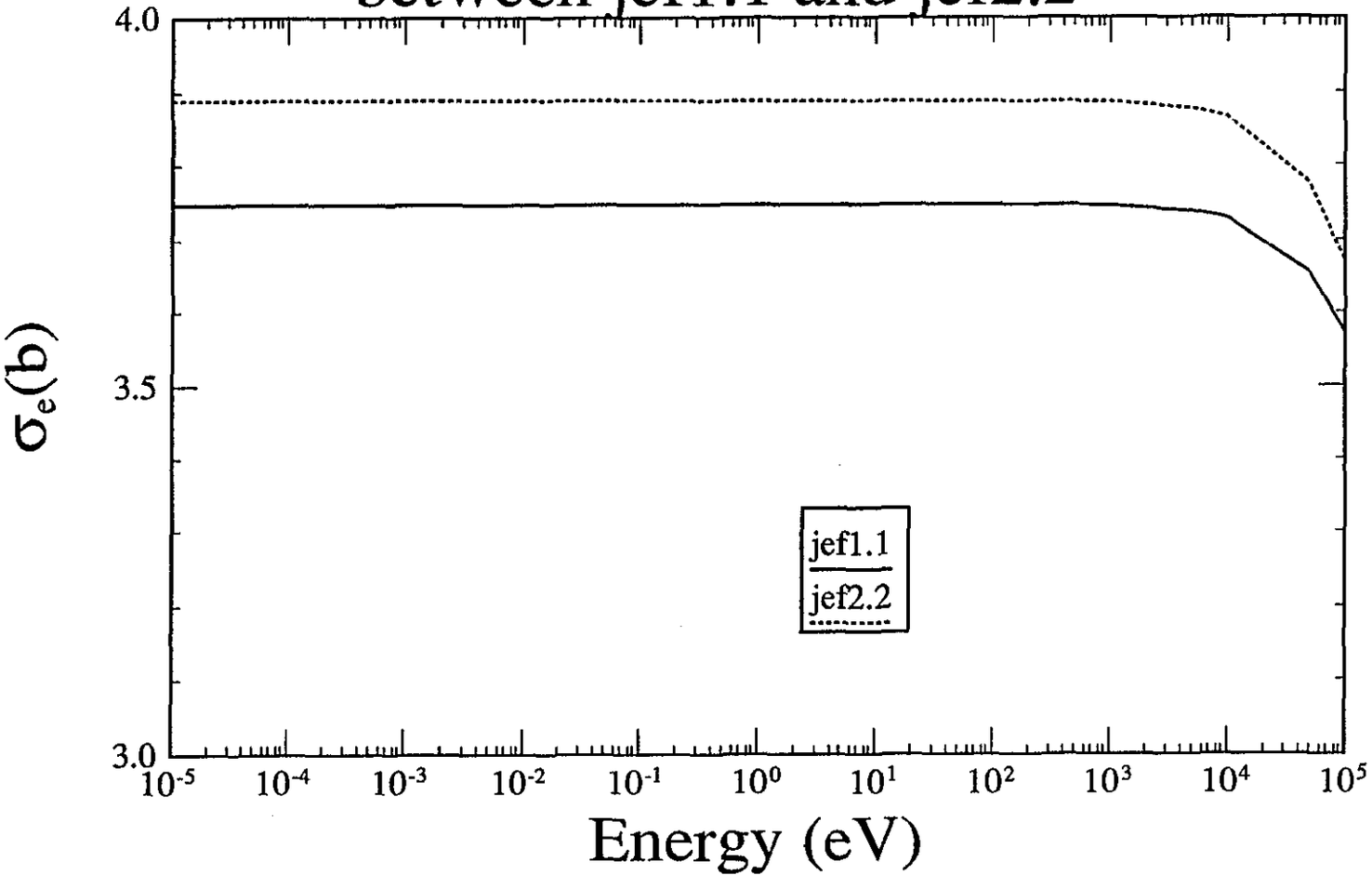

TempleGraph 2.3, Origin: /home/zahir/ywang@zahir - Fri Jul 30 10:33:12 1993 (data file was o16els)

Figure 10 : Comparison of σ_e for ^{16}O between jef1.1 and jef2.2

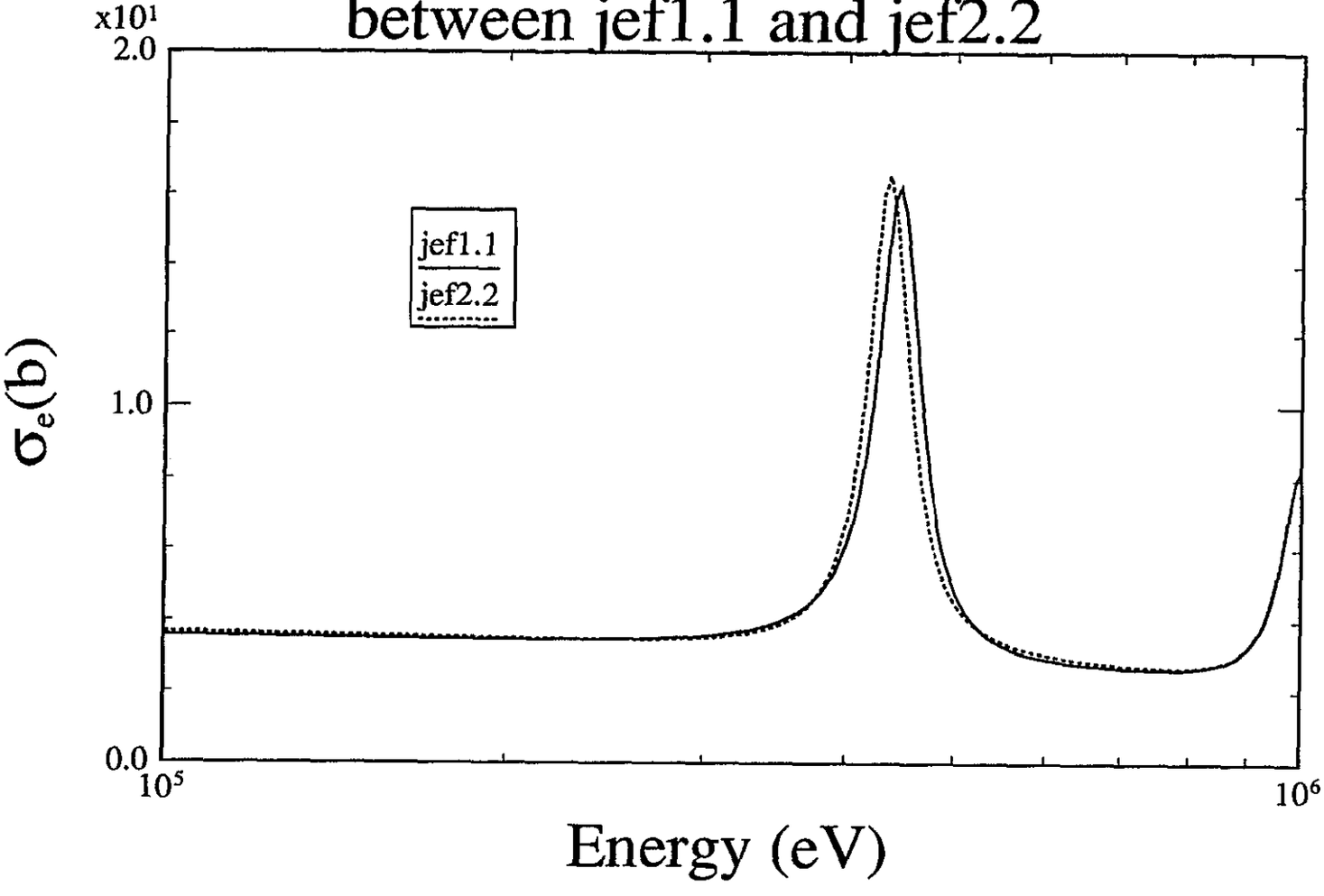

TempleGraph 2.3, Origin: /home/zahir/ywang@zahir - Fri Jul 30 10:45:45 1993 (data file was o16els)

Figure 10 : Comparison of σ_e for ^{16}O between jef1.1 and jef2.2

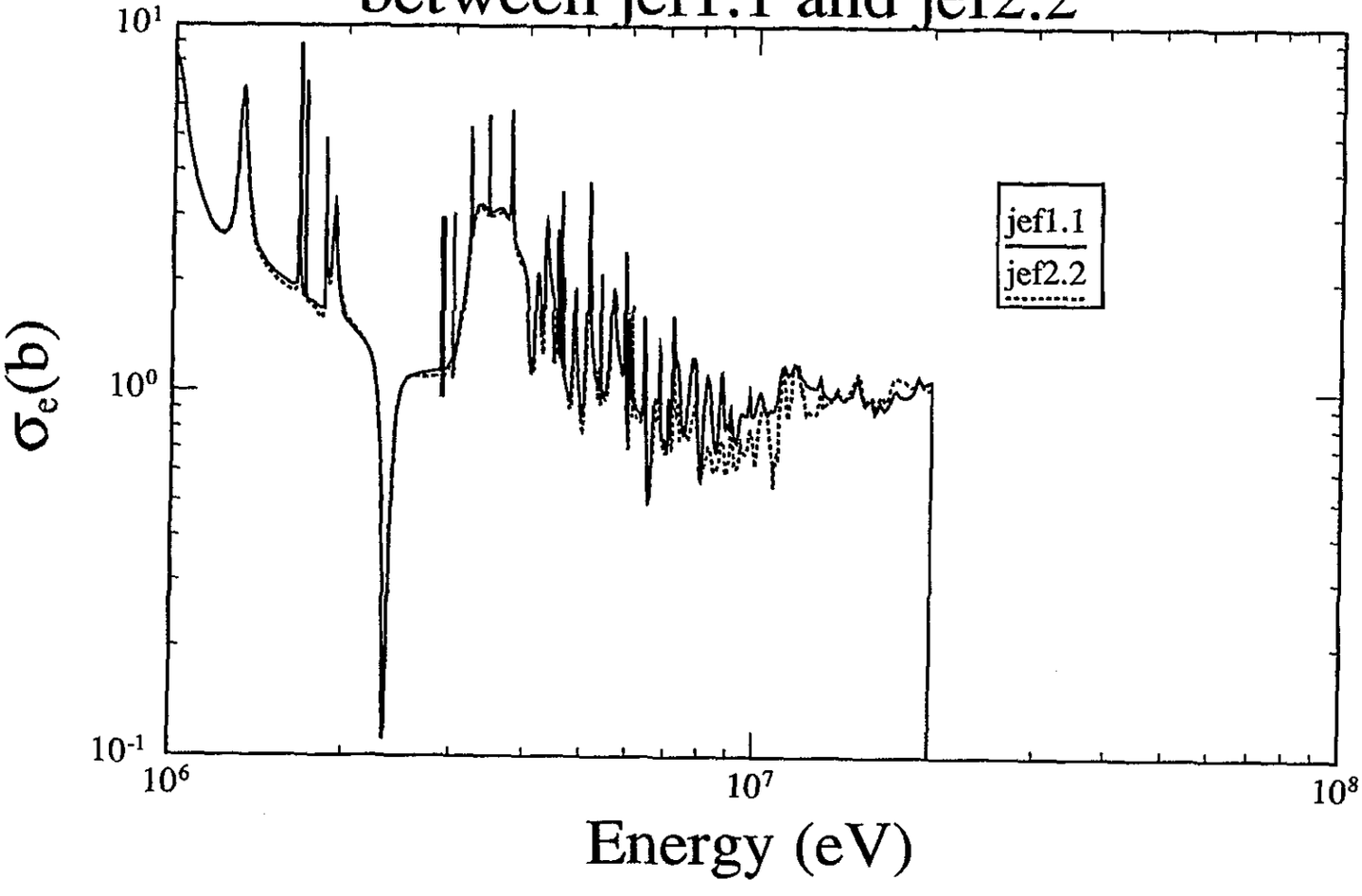

TempleGraph 2.3, Origin: /home/zahir/ywang@zahir - Fri[illegible] 30 10:53:27 1993 (data file was o16els)

Figure 11 : Comparison of TRX-1 Cell-Spectra Calculated with Different Libraries

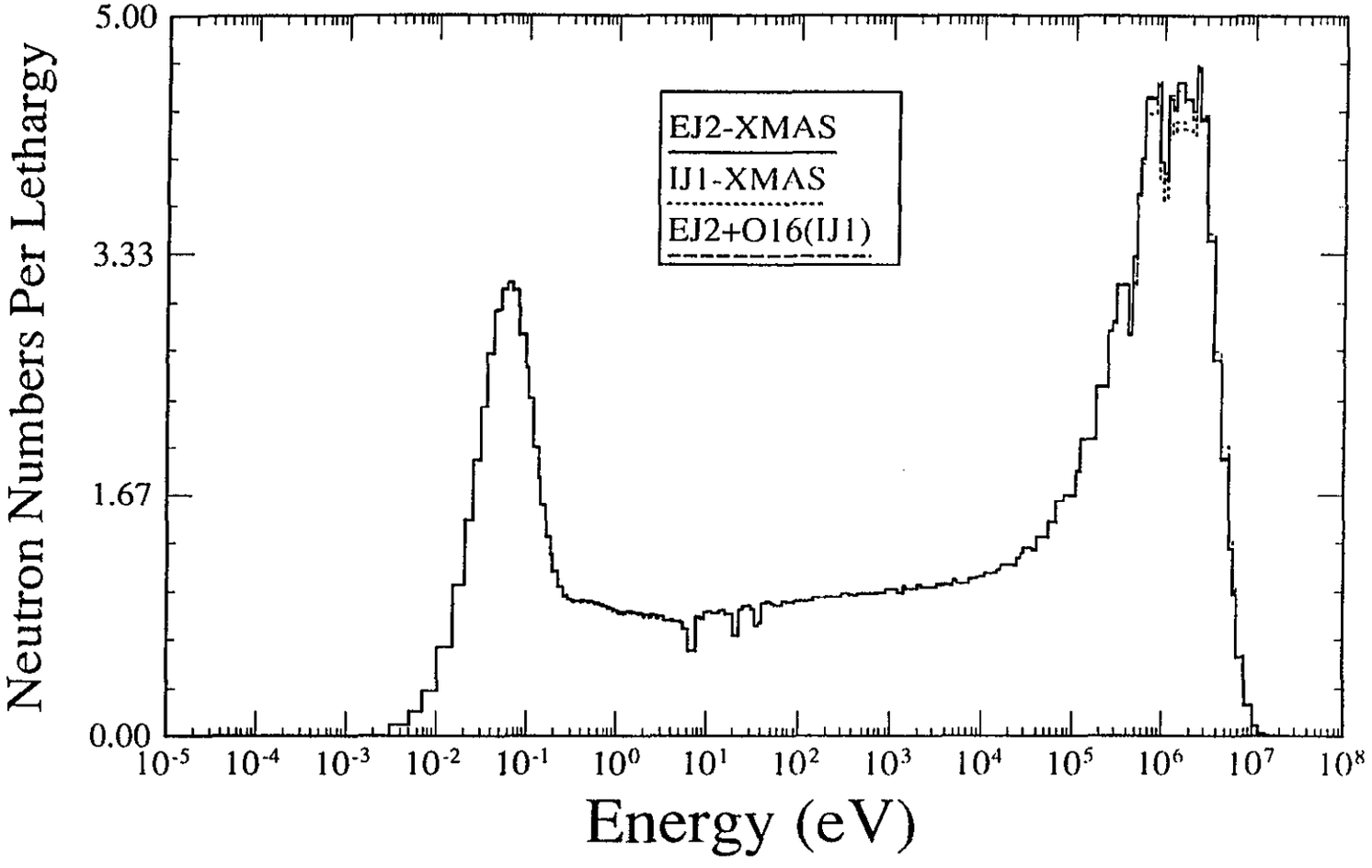

TempleGraph 2.3, Origin: /home/zahir/ywang@crypton - Wed Aug 11 12:29:14 1993 (data file was ctr1bccp2)

Figure 12 : Comparison of TRX-1 Full Core-Spectra Calculated with Different Libraries

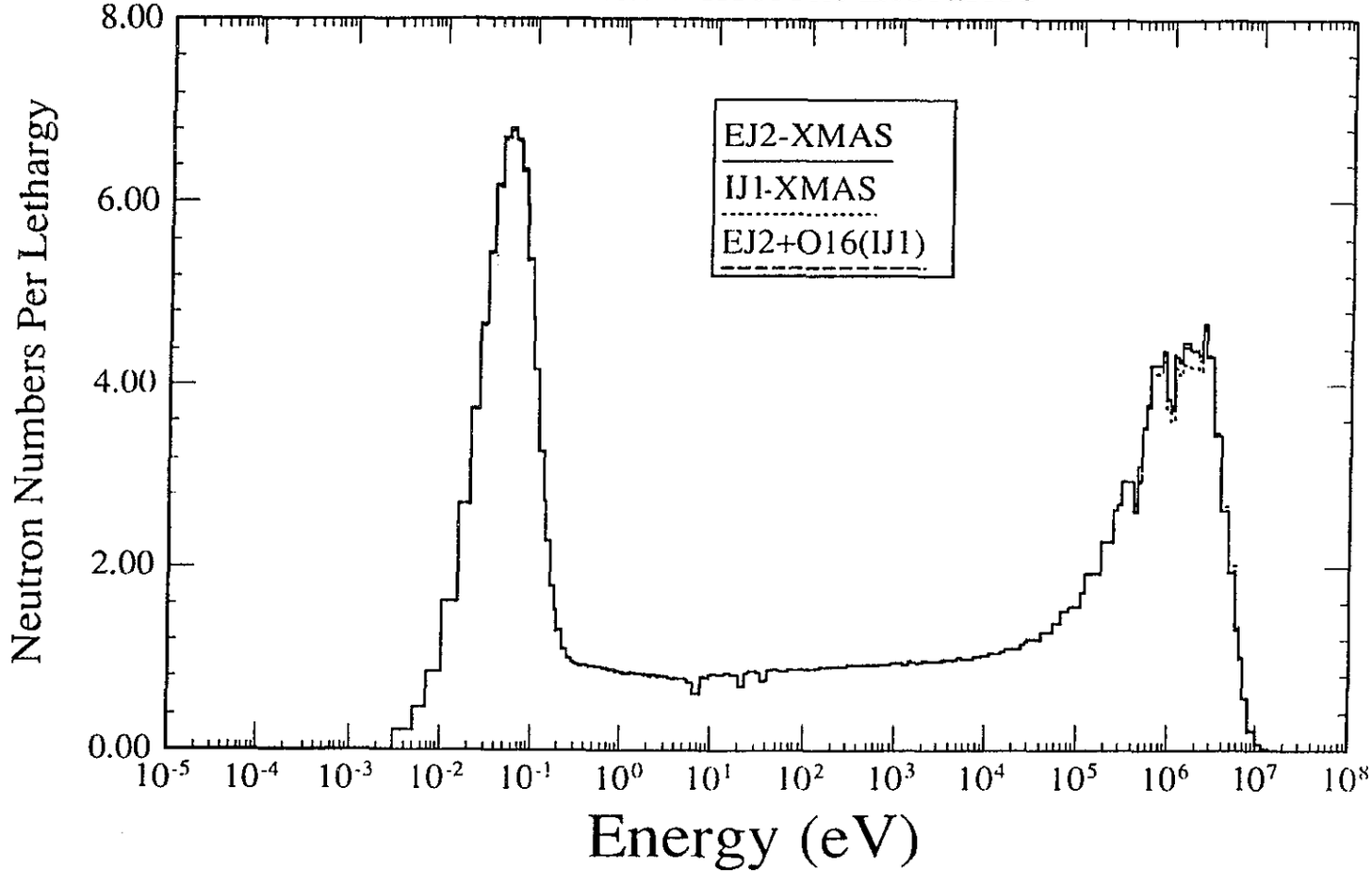

TempleGraph 2.3, Origin: /home/zahir/yw[redacted]@crypton - Wed Aug 11 13:57:07 1993 (data file was ct[redacted]op2)